Hydrazine-Assisted, Low-Temperature Aerosol Pyrolysis Method to Synthesize γ-Fe_2O_3

Soubir Basak,[†] Koyar S. Rane,[‡] and Pratim Biswas*,[†]

Aerosol and Air Quality Research Laboratory, Department of Energy, Environmental and Chemical Engineering, Washington University in Saint Louis, Saint Louis, Missouri 63130, and Department of Chemistry, Goa University, India

Received January 5, 2008. Revised Manuscript Received May 5, 2008

Oxides of iron in different crystalline forms such as hematite, maghemite, and magnetite have been used in number of industrial and biomedical applications in recent years. These materials are often synthesized in multiple-step processes in which simultaneous control of particle size, shape, morphology, and crystallinity is difficult. A single-step, low-temperature spray pyrolysis of iron precursors with hydrazine in a furnace aerosol reactor (FuAR) is described. To help select viable precursors and guide selection of operating conditions for the aerosol process, hydrazine derivatives of iron precursors are prepared in batch and analyzed with TGA, FTIR, and XRD. These results were also used to identify the chemical formula of hydrazinated precursors and elucidate the reaction pathway for the precursors such as ferrous acetate, ferric nitrate, and ferrous oxalate that are suitable for single-step aerosol reactor synthesis. These iron precursors are aerosolized and reacted in situ with hydrazine vapor to demonstrate the single-step, low-temperature production of metarstable γ-Fe_2O_3. Structurally similar cubic intermediates (FeO, Fe_3O_4, γ-$FeOOH \cdot H_2O$) are the key decomposition intermediates observed during the synthesis of γ-Fe_2O_3. It is shown that hydrazinated iron precursors decompose at a lower temperature compared to the same unhydrazinated precursors to produce pure γ-Fe_2O_3. The localized exothermal reaction of hydrazine released from the hydrazinated precursor with oxygen along with a controlled supply of energy assists in the production of the metastable γ-Fe_2O_3. Hydrazine oxidation releases moisture and nitrogen as reaction byproduct, which further enhances the stability of γ-Fe_2O_3.

1. Introduction

Oxides of iron have diverse crystal structures and hence varying properties, and they find use in a variety of technological applications. Hematite (α-Fe_2O_3), which has a hexagonal corrundum structure, finds applications in catalysis, as a sorbent for toxic gas removal, and in the pigment industry.[1–3] Magnetite (Fe_3O_4), which is cubic iron oxide with an inverse spinel structure, is used as a catalyst for ammonia synthesis, as a sorbent for heavy metal removal, and for tissue engineering.[4–6] Maghemite (γ-Fe_2O_3), which is a vacancy ordered cubic spinel, has applications in magnetic recording and information storage devices, ferrofluid, catalyst, gas sensors, biosensors, and in magneto-optical devices.[7–12] The use of iron oxides, especially spherically shaped Fe_3O_4 and γ-Fe_2O_3, has seen tremendous growth in the biomedical field because of their superior chemical and thermal stability, hardness, non-toxicity, nonradioactivity, and biocompatibility.[13,14] They have been studied for use as image intensifying agents in nuclear magnetic resonance imaging (MRI),[14–16] medical diagnosis,[17] controlled drug delivery,[18] magnetic-induced cancer therapy (hyperthermia),[19,20] and biomedical heating applications.[21]

The control of size, shape, morphology, and crystallinity of iron oxides are crucial factors that determine their

* Corresponding author: Tel: (314) 935-5482. Fax: (314) 935-5464. E-mail: pratim.biswas@wustl.edu.
[†] Washington University in Saint Louis.
[‡] Goa University.

(1) Wu, B.; Tian, L.; Xiang, H.; Zhang, Z.; Li, Y. W. *Catal. Lett.* **2005**, *104* (3−4), 211–218.
(2) Waychunas, G. A.; Kim, C. S.; Banfield, J. F. *J. Nanopart. Res.* **2005**, *7* (4−5), 409–433.
(3) Potter, M. J. Iron Oxide Pigments. In *U.S. Geological Survey Minerals Year Book*; U.S. Geological Survey: Reston, VA, 2001.
(4) Guan, S.; Lin, H. Z. *Ind. Eng. Chem. Res.* **2000**, *39* (8), 2891–2895.
(5) Yean, S.; Cong, L.; Yavuz, C. T.; Mayo, J. T.; Yu, W. W.; Kan, A. T.; Colvin, V. L.; Tomson, M. B. *J. Mater. Res.* **2005**, *20* (12), 3255–3264.
(6) Ito, A.; Shinkai, M.; Honda, H.; Kobayashi, T. *J. Biosci. Bioeng.* **2005**, *100* (1), 1–11.
(7) Hayes, B. *Am. Sci.* **2002**, *90* (3), 212–216.
(8) Bacri, J.-C.; Silva, M. d. F. D.; Perzynski, R.; Pons, J.-N.; Roger, J.; Sabolovic, D.; Halbreich, A. *Use of Magnetic Nonoparticles for Thermolysis of Cells in a Ferrofluid*; Plenum Press: New York, 1997.
(9) Teng, X. W.; Black, D.; Watkins, N. J.; Gao, Y. L.; Yang, H. *Nano Lett.* **2003**, *3* (2), 261–264.
(10) Jing, Z.; Wang, Y.; Wu, S. *Sens. Actuators, B* **2006**, *113*, 177–181.
(11) Perez, J. M.; Josephson, L.; Weissleder, R. *Chembiochem* **2004**, *5* (3), 261–264.
(12) Ilievski, F.; Tepper, T.; Ross, C. A. *IEEE Trans. Magn.* **2003**, *39* (5), 3172–3174.
(13) Schneeweiss, O.; Zboril, R.; Pizurova, N.; Mashlan, M.; Petrovsky, E.; Tucek, J. *Nanotechnology* **2006**, *17* (2), 607–616.
(14) Frank, J. A.; Zywicke, H.; Jordan, E. K.; Mitchell, J.; Lewis, B. K.; Miller, B.; Bryant, L. H.; Bulte, J. W. M. *Acad. Radiol.* **2002**, *9*, S484−S487.
(15) Lanza, G. M.; Winter, P. M.; Caruthers, S. D.; Morawski, A. M.; Schmieder, A. H.; Crowder, K. C.; Wickline, S. A. *J. Nucl. Cardiol.* **2004**, *11* (6), 733–743.
(16) Arbab, A. S.; Yocum, G. T.; Kalish, H.; Jordan, E. K.; Anderson, S. A.; Khakoo, A. Y.; Read, E. J.; Frank, J. A. *Blood* **2004**, *104* (4), 1217–1223.
(17) Pankhurst, Q. A.; Connolly, J.; Jones, S. K.; Dobson, J. *J. Phys. D: Appl. Phys.* **2003**, *36* (13), R167−R181.

10.1021/cm800034g CCC: $40.75
Published on Web 07/17/2008

applicability. As these properties are a strong function of the synthesis methodology, considerable research has been performed on the preparation of these oxides by solvothermal and sol−gel methods starting from simple compounds like chlorides, nitrates, sulfates, carboxylates, alkoxides, and carbonyls.[22–28] Although these are low-temperature synthesis routes, most of them involve multiple steps and the synthesized materials often contain impurities such as unreacted or partially reacted surfactants. Heat-releasing additives such as hydrazine, urea, and glycine have been used in combustion syntheses in solid phase and solvothermal methods for the preparation of many value-added engineered materials.[29–32] The importance of hydrazine complexes in the formation of perovskite,[32] ceria,[33] cobaltites,[34] and spinel ferrites[35,36] is that they lead to a considerable reduction in the decomposition temperature. The control of the product crystallinity using batch pyrolysis processes by adjusting the heating rate, fuel to oxidizer ratio, type of fuel has been demonstrated. However, it is difficult to control particle size and morphology by this method. In contrast, aerosol route synthesis processes such as spray pyrolysis using soluble iron compounds like nitrates,[37] chlorides,[38] or highly volatile iron pentacarbonyl[39] as starting materials have been demonstrated to produce high-purity, unagglomerated, spherical-shaped submicrometer- to nanometer-sized iron oxide particles by adequately tuning the process parameters (like precursor flow rate, concentration of the metal ions, decomposition atmosphere, and temperature). The thermal products of these decomposable salts and complexes of iron are primarily the thermodynamically stable α-Fe_2O_3. The challenge is to synthesize metastable γ-Fe_2O_3 with a well-controlled size, shape, and morphology using an economically viable process like spray pyrolysis. However, the combination of heat-releasing additives with iron precursors in aerosol processes has not been demonstrated.

The present investigation relates to the synthesis of γ-Fe_2O_3 by a single step low-temperature, gas-phase aerosol pyrolysis method in a furnace aerosol reactor (FuAR) using hydrazine as an additive. The strong reducing power, monodented ligand property, ability to scavenge oxygen, and formation of moisture and nitrogen as decomposition byproducts are the key advantages to consider hydrazine as a potential additive, in comparison to other alternates such as urea and glycine. Modified precursors prepared in a batch method by equilibrating the solid phase iron compounds in a hydrazine atmosphere are used to identify the chemical composition of the hydrazinated compound, understand the decomposition mechanism, identify the key reaction intermediates and determine the operating conditions suitable for the aerosol pyrolysis process. On the basis of the results of the batch studies, single-step aerosol processes with hydrazination are demonstrated for the production of metastable γ-Fe_2O_3. The details of hydrazine-assisted, gas-phase, low-temperature aerosol pyrolysis of these iron compounds and their hydrazine complexes are discussed.

2. Experimental Section

Detailed results of reaction of hydrazine with iron precursors that are necessary for design of aerosol processes are not available in the literature. A series of iron precursors were initially reacted with hydrazine and analyzed to identify the chemical composition of the hydrazinated adduct and the suitable operating conditions for aerosol synthesis process. Using the findings of the batch studies, we carried out a detailed study of aerosolized iron precursors to produced iron oxides. Although several other iron precursors (such as ferrous sulfate, ferric acetylacetonate, ferric chloride) were studied using the batch process, only the results for precursors found suitable for aerosol spray pyrolysis are presented.

2.1. Materials: Iron Oxide Precursors. Commercial iron compound precursors with a variety of physical and chemical properties were chosen based on their solubility, availability, stability, and oxidizing properties. Ferrous acetate, $Fe(CH_3COO)_2$ (soluble in water), and ferric nitrate, $Fe(NO_3)_3 \cdot 9H_2O$ (strong oxidizing agent, highly soluble in water), were used as-received. Ferrous oxalate, $FeC_2O_4 \cdot 2H_2O$ (insoluble in water), however, was prepared by a wet precipitation method, by adding a slight excess of oxalic acid to a hot dilute aqueous solution of ferrous chloride. The micrometer- sized yellow acicular crystals of $FeC_2O_4 \cdot 2H_2O$, after being washed several times with water, were collected on filter paper and dried in silica desiccators.

2.2. Batch Study. Hydrazination of the iron precursors were performed by a literature-reported equilibration method[29–32,40–43]

(18) Pulfer, S. K.; Ciccotto, S. L.; Gallo, J. M. *J. Neuro-Oncol.* **1999**, *41* (2), 99–105.
(19) Gangopadhyay, P.; Gallet, S.; Franz, E.; Persoons, A.; Verbiest, T. *IEEE Trans. Magn.* **2005**, *41* (10), 4194–4196.
(20) Chastellain, M.; Petri, A.; Gupta, A.; Rao, K. V.; Hofmann, H. *Adv. Eng. Mater.* **2004**, *6* (4), 235–241.
(21) Dutz, S.; Hergt, R.; Murbe, J.; Topfer, J.; Muller, R.; Zeisberger, M.; Andra, W.; Bellemann, M. E. *Z. Phys. Chem.* **2006**, *220* (2), 145–151.
(22) Chen, D.; Xu, R. *Mater. Res. Bull.* **1998**, *33* (7), 1015–1021.
(23) Khaleel, A. A. *Chem.−Eur. J.* **2004**, *10* (4), 925–932.
(24) Jing, Z. H.; Wu, S. H. *J. Solid State Chem.* **2004**, *177* (4−5), 1213–1218.
(25) Rane, K. S.; Verenkar, V. M. S. *Bull. Mater. Sci.* **2001**, *24* (1), 39–45.
(26) Maruyama, T.; Shinyashiki, Y. *Thin Solid Films* **1998**, *333* (1−2), 203–206.
(27) Woo, K.; Hong, J.; Choi, S.; Lee, H. W.; Ahn, J. P.; Kim, C. S.; Lee, S. W. Easy synthesis and magnetic properties of iron oxide nanoparticles. *Chem. Mater.* **2004**, *16* (14), 2814–2818.
(28) Venkataraman, A.; Mukhedkar, V. A.; Mukhedkar, A. J. *J. Therm. Anal.* **1989**, *35* (7), 2115–2124.
(29) Jacob, K. T.; Verman, R.; Mallya, R. M. *J. Mater. Sci.* **2002**, *37* (20), 4465–4472.
(30) Zhan, J. H.; Xie, Y.; Yang, X. G.; Zhang, W. X.; Qian, Y. T. *J. Solid State Chem.* **1999**, *146* (1), 36–38.
(31) Kim, J. Y.; Sriram, M. A.; McMichael, P. H.; Kumta, P. N.; Phillips, B. L.; Risbud, S. H. *J. Phys. Chem. B* **1997**, *101* (24), 4689–4696.
(32) Azegami, K.; Yoshinaka, M.; Hirota, K.; Yamaguchi, O. *Mater. Res. Bull.* **1998**, *33* (2), 341–348.
(33) Heintz, J. M.; Bernier, J. C. *J. Mater. Sci.* **1986**, *21* (5), 1569–1573.
(34) Patil, K. C.; Gajapathy, D.; Verneker, V. R. P. *J. Mater. Sci. Lett.* **1983**, *2* (6), 272–274.
(35) Patil, K. C.; Gajapathy, D.; Kishore, K. *Thermochim. Acta* **1982**, *52* (1−3), 113–120.
(36) Patil, K. C.; Gajapathy, D.; Pai Verneker, V. R. *Mater. Res. Bull.* **1982**, *17*, 29–32.
(37) Basak, S.; Chen, D. R.; Biswas, P. *Chem. Eng. Sci.* **2007**, *64* (4), 1263–1268.
(38) Desai, J. D.; Pathan, H. M.; Min, S. K.; Jung, K. D.; Joo, O. S. *Appl. Surf. Sci.* **2006**, *252* (23), 8039–8042.
(39) McMillin, B. K.; Biswas, P.; Zachariah, M. R. *J. Mater. Res.* **1996**, *11* (6), 1552–1561.
(40) Borker, V.; Rane, K. S.; Dalal, V. N. K. *J. Mater. Sci.: Mater. Electron.* **1993**, *4* (3), 241–248.
(41) Rane, K. S.; Verenkar, V. M. S.; Pednekar, R. M.; Sawant, P. Y. *J. Mater. Sci.: Materi. Electron.* **1999**, *10* (2), 121–132.
(42) Rane, K. S.; Verenkar, V. M. S.; Sawant, P. Y. *J. Mater. Sci.: Mater. Electron.* **1999**, *10* (2), 133–140.
(43) Schmidt, E. W., *Hydrazine and its Derivatives: Preparation, Properties, Applications*, 2nd ed.; John Wiley & Sons: New York, 2001.

Table 1. Overall Test Plan for the Experiments: Batch Studies with Results of Decomposition Temperature, Final Weight Loss, Hydrazine Content, and Crystal Phase (Test 1–12) and Aerosol Pyrolysis with Hydrazine As a Reactant (Test 13–26)

test ID	precursor	decomposition environment	decomposition temperature (°C)	obsd weight loss (%) (theoretical)	obsd N_2H_4 content by KIO_3 titration (%) (theoretical)	composition (from XRD)
1	$Fe(CH_3COO)_2$	air	300	56.5(54.3)		Fe_3O_4 + α-Fe_2O_3
2		nitrogen	340	56.0(54.3)		Fe_3O_4
3	$Fe(CH_3COO)_2 \cdot 2N_2H_4$	air	320	65.9(66.4)	27.3(26.8)	γ-Fe_2O_3
4		nitrogen	340	65.0(66.4)	27.3(26.8)	Fe_3O_4
5	$Fe(NO_3)_3 \cdot 9H_2O$	air	300	79.9(80.2)		α-Fe_2O_3
6		nitrogen	300	79.9(80.2)		α-Fe_2O_3
7	$Fe(NO_3)_3 \cdot 9H_2O$ with hydrazine	air	300	79.9(26.7)		α-Fe_2O_3
8		nitrogen	300	79.9(26.7)		α-Fe_2O_3
9	$FeC_2O_4 \cdot 2H_2O$	air	260	54.4(55.6)		α−Fe_2O_3
10		nitrogen	300	56.2(55.6)		Fe_3O_4 + FeO
11	$FeC_2O_4 \cdot 2N_2H_4$	air	150	61.2(61.7)	31.4(30.7)	γ-Fe_2O_3
12		nitrogen	430	61.4(61.7)	31.4(30.7)	Fe_3O_4 + FeO

test ID	precursor	carrier gas	furnace temperature (°C)	precursor concentration (M)	combustion fuel used	composition (from XRD)
13	$Fe(CH_3COO)_2$	nitrogen	300	0.1	N_2H_4	amorphous + Fe_3O_4
14		nitrogen	500	0.1	N_2H_4	Fe_3O_4
15		air	500	0.1	N_2H_4	γ-Fe_2O_3, α-Fe_2O_3
16	$Fe(NO_3)_3 \cdot 9H_2O$	air	100	0.1	−	[a] $FeOOH \cdot H_2O$
17		air	100	0.1	N_2H_4	$N_2H_5NO_3$, γ-$FeOOH \cdot H_2O$
18		air	300	0.1	N_2H_4	$N_2H_5NO_3$, γ-$FeOOH \cdot H_2O$
19		nitrogen	400	0.1	N_2H_4	γ-Fe_2O_3
20		nitrogen	450	0.1	N_2H_4	γ-Fe_2O_3
21		air	450	0.1	N_2H_4	γ-Fe_2O_3
22		nitrogen	550	0.1	N_2H_4	γ-Fe_2O_3
23		nitrogen	550	0.01	N_2H_4	γ-Fe_2O_3
24[b]		air	800	0.1		α-Fe_2O_3
25[c]	$FeC_2O_4 \cdot 2N_2H_4$	air	400			γ-Fe_2O_3
26[c]		nitrogen	500			Fe_3O_4

[a] From TGA analysis. [b] Use of diffusion drier just before the furnace reactor. [c] Due to low solubility in water or any other known solvent, these samples are aerosolized using a fluidizer.

for the batch study. The powders of the iron compounds were spread on a Petri dish and introduced into a close chamber reactor at room temperature that contained 98% pure hydrazine monohydrate, $N_2H_4 \cdot H_2O$ (Fluka). The hydrazine vapor in the chamber (vapor pressure of hydrazine is 14.4 Torr at 25 °C) reacted with the iron precursors to form the hydrazinated iron compounds or adducts.

Hydrazinated iron precursors were first examined by thermogravimetric analysis (TGA, TA Instrument, model 2950) to identify weight loss at different temperatures and determine the final decomposition temperature in both air and nitrogen atmospheres (30−600 °C at a heating rate of 10 °C min^{-1}). Isothermal decomposition of these precursors was then carried out in a muffle furnace (for 1 h) at the final decomposition temperature found from TGA studies for crystallographic characterization of decomposed products by powder X-ray diffractometry (XRD, Rigaku D-MAX/A diffractometer with Cu Kα radiation, $\lambda = 1.5418$ Å). Hydrazine uptake by the iron precursor compound was estimated by direct titration of the compounds against a standard KIO_3 solution.[44] The hydrazinated iron compounds were characterized by the shift in bond stretching frequency in the infrared region using a Fourier transform infrared spectrometer (FTIR) (model Nexus-470, Thermo Nicolet) by mixing the sample with KBr (1:20 ratio). The main purpose of the batch study is to identify conditions suitable for production of γ-Fe_2O_3 in the aerosol pyrolysis method along with understanding of the decomposition mechanism. The complete test plan along with the chemical formula of hydrazinated precursors, final weight loss (by thermogravimetric analysis), hydrazine content (by KIO_3 titration), and crystal phases (as identified by XRD analysis) are summarized in Table 1.

2.3. Aerosol Pyrolysis Study. The experimental setup for thermal decomposition of the iron oxide precursors in the aerosol reactor consisted of three components: a nebulizer/fluidizer as a precursor feeder, a tubular furnace, and an electrostatic precipitator (ESP). The schematic diagram of the furnace aerosol reactor (FuAR) is shown in Figure 1. An aqueous solutions of ferrous acetate (0.1 M) and ferric nitrate (0.01−0.1 M) were aerosolized using a nebulizer (TSI, model 3076) at 20 psi pressure, whereas a fluidizer was used to feed solid ferrous oxalate and its hydrazine derivative. Another nebulizer (TSI, model 3076, 20 psi pressure) was used to aerosolize hydrazine monohydrate. The aerosolized precursor and hydrazine were mixed and reacted in a 1 m long preheater tube to ensure complete hydrazination. The temperature of the preheater tube was maintained at 100 °C, below the thermodynamic decomposition temperature of the hydrazinated adduct (e.g., the thermodynamic decomposition temperature of $N_2H_5NO_3$ is 120 °C). The aerosol was then decomposed in the tubular furnace aerosol reactor (FuAR) (Lindbergh BlueM, model STF54779C) at different temperatures (100−800 °C). The temperature of the preheater and the furnace reactor was precisely controlled within ±5 °C using temperature controllers (Thermolyne, model BSAT101−040, and Lindbergh BlueM, model CC58485C) and was calibrated with a thermocouple system. At steady state, the gas flowing through the system was at the set point temperature of the individual controller. Air was used as carrier gas to maintain an oxidizing atmosphere,

(44) Vogel, I. A. *A Text Book of Quantitative Inorganic Analysis*, 4th ed.; Longmans ELBS: London, 1978.

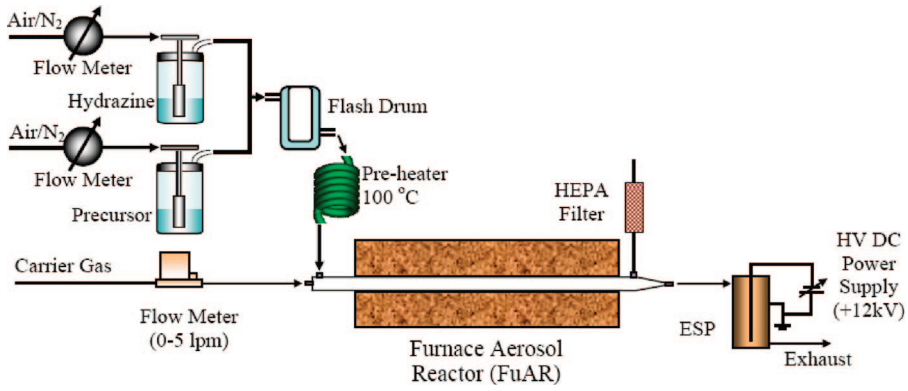

Figure 1. Schematic diagram of the experimental system to synthesize metal oxide nanomaterials using an aerosol hydrazine-assisted combustion method.

whereas nitrogen was used to provide an inert atmosphere inside the reactor. The synthesized particles were collected on a cylindrical electrostatic precipitator (ESP) with an applied potential of +12 kV at room temperature. The ESP was used for its high collection efficiency and the ability to handle a large volume of gas at elevated temperatures, with a very low pressure drop for continuous operation. A positive potential was applied to minimize ozone formation in the ESP. The microstructures of the decomposed products were observed by a scanning electron microscope (SEM, model Hitachi S-4500).

The temperature and the decomposition environment in the furnace aerosol reactor are selected based on the results of the batch studies to optimize the formation of γ-Fe_2O_3 and minimize the number of test runs. Control of particle size is demonstrated by varying the concentration of the precursor and using a diffusion drier before the furnace. The overall test plan along with the product composition for aerosolized decomposition study is listed in Table 1.

3. Results

Hydrazinated iron precursors prepared by the batch method were analyzed to establish the decomposition temperature and reaction mechanism to facilitate the synthesis of γ-Fe_2O_3 by the aerosol spray pyrolysis method. Batch studies allow the testing of several precursors, and results for only the three with the potential for success in the single-step aerosol method are presented.

3.1. Batch Studies. *3.1.1. Ferrous Acetate.* The isothermal weight loss for ferrous acetate carried out in a TGA (Figure 2a) indicates 56.5% total weight loss in air and 56.0% in nitrogen (Table 1). The theoretical total weight loss calculated for decomposition of $Fe(CH_3COO)_2$ to Fe_2O_3 amounts to 54.3% and 55.4% when Fe_3O_4 is the final product. The final products collected by decomposing ferrous acetate at ~300 °C in air is found to be a mixture of Fe_2O_3 (ICCD: 00−033−0664) and Fe_3O_4 (ICCD: 01−072−8152) (Test 1) and pure Fe_3O_4 at ~340 °C in nitrogen (Test 2) as identified by XRD (Figure 3).

Ferrous acetate equilibrated with hydrazine resulted in a weight loss of 65.9% at ~320 °C in air (Test 3) and 65.0% at 340 °C in nitrogen (Test 4). A careful observation of the TGA traces indicated that the hydrazinated sample resulted in a sharp weight loss at ~120 °C in air (completing >90% loss), whereas all other samples decomposed at higher temperatures. The XRD pattern of the thermal product in air at 320 °C (Figure 3) was maghemite (ICCD: 00−025−1402), whereas in nitrogen, magnetite was the end product. The hydrazine estimation done by KIO_3 titration showed that the complex had 27.3% N_2H_4. Considering the total loss of the acetate complex observed in air and nitrogen, the formula $Fe(CH_3COO)_2 \cdot 2N_2H_4$ is proposed. The total weight loss and N_2H_4 content of 26.8% calculated from the proposed formula closely matches the experimental values. Fe_3O_4 is the final product in nitrogen environment while oxygen is necessary for synthesis of γ-Fe_2O_3 and α-Fe_2O_3. The following reaction scheme is proposed where formation of γ-Fe_2O_3 is preceded by structurally similar intermediate (Fe_3O_4), which is then converted to α-Fe_2O_3 by heat treatment.

$$Fe(CH_3COO)_2 \cdot 2N_2H_4 \xrightarrow{-2N_2H_4} Fe(CH_3COO)_2 \rightarrow Fe_3O_4 \xrightarrow{+O_2} \gamma\text{-}Fe_2O_3 \xrightarrow{\Delta} \alpha\text{-}Fe_2O_3$$

The infrared (IR) bands for ferrous acetate (Figure S1 in the Supporting Information) has a $\nu_{asym(COO)}$ band positioned at ~1600 cm^{-1} and $\nu_{sym(COO)}$ at ~1400 cm^{-1}. A broad band in the region 3500−3000 cm^{-1} is due to $\nu_{(OH)}$ of adsorbed water. The hydrazine complex, on the other hand, has a band centered at ~3300 cm^{-1} due to $\nu_{(NH)}$ and other at ~950 cm^{-1} due to $\nu_{(NN)}$. The metal−nitrogen bond in hydrazine complexes are in general formed in these regions[45] and other band positions of acetate are observed in the usual positions. The IR studies thus confirmed the hydrazine linked with the ferrous acetate.

3.1.2. Ferric Nitrate. Ferric nitrate decomposes in multiple steps, both in air (Test 5) and nitrogen (Test 6), and the observed total TGA weight loss (Figure 2b) of 79.9% (Table 1) matched well with the expected loss of 80.2% giving an end product of α-Fe_2O_3. The formation of α-Fe_2O_3 at 300 °C was confirmed by batch decomposition in muffle furnace in both air and nitrogen atmosphere by XRD analysis (Figure 3). The inflection in the TGA curve between 30 and 120 °C with ~26.7% weight loss accounts for the removal of six H_2O molecules to form $Fe(NO_3)_3 \cdot 3H_2O$. The other inflection point at ~190 °C with ~77.8% weight loss indicates the

(45) Braibanti, A.; Dallavalle, E.; Pellinghelli, M. A.; Leporati, E. *Inorg. Chem.* **1968**, *7* (7), 1430–1433.

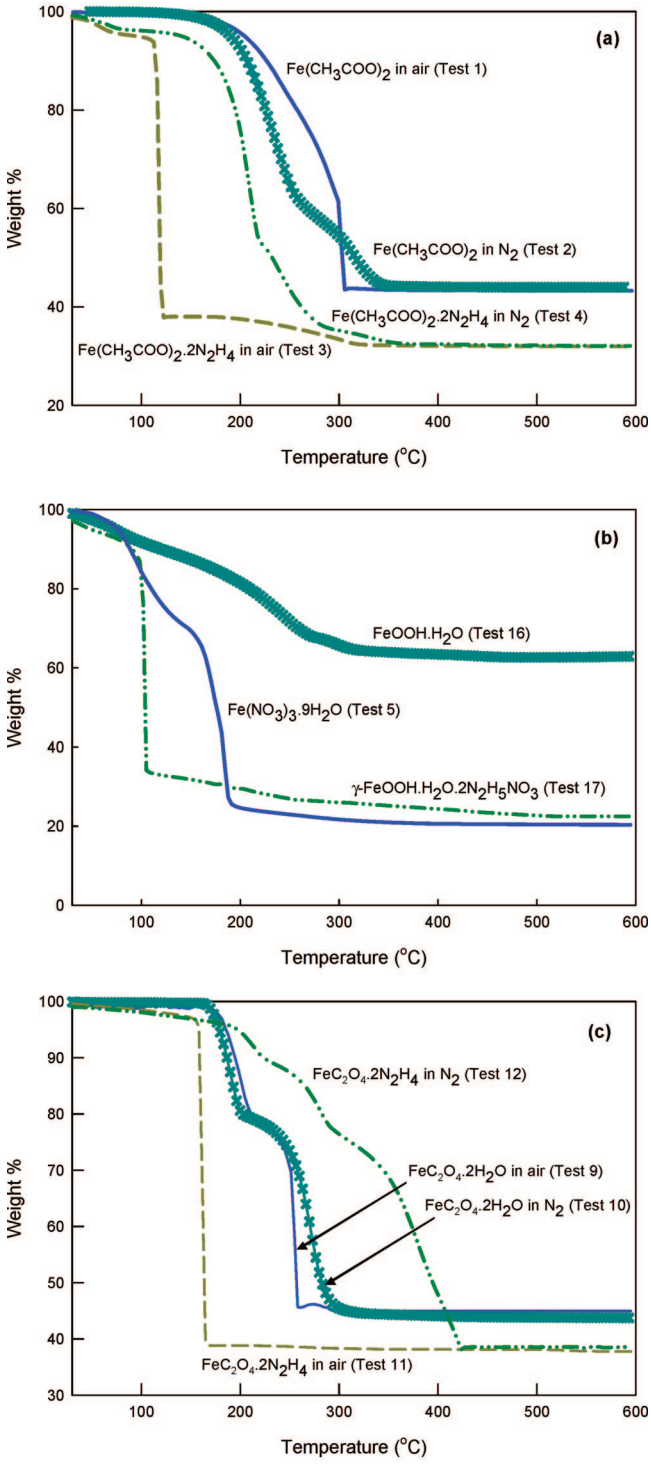

Figure 2. Characteristic thermogravimetric traces of (a) ferrous acetate and its hydrazinate, (b) ferric nitrate and its hydrazinate, and (c) ferrous oxalate and its hydrazinate.

formation of goethite type (α-FeOOH·H_2O) intermediate, which is also confirmed by other reports in the literature by Mäossbauer and XRD analysis during a similar wet chemical synthesis process.[46,47] Unlike ferrous acetate system, α-Fe_2O_3 is always obtained as end product for ferric nitrate system regardless of decomposition atmosphere. Formation of α-Fe_2O_3 is preceded by the structurally similar intermediate (α-FeOOH·H_2O) intermediates as depicted below

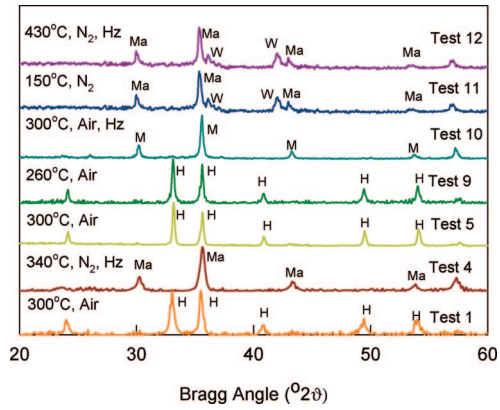

Figure 3. Characteristic X-ray diffraction patterns of the samples collected during decomposition studies of various precursors (H, hematite; M, magnetite; Ma, maghemite; W, wurtzite; Hz, with hydrazine condition).

$$Fe(NO_3)_3{\cdot}9H_2O \xrightarrow{-6H_2O} Fe(NO_3)_3{\cdot}3H_2O \xrightarrow{3HNO_3}$$

$$\alpha\text{-}FeOOH{\cdot}H_2O \xrightarrow{H_2O} \alpha\text{-}Fe_2O_3$$

The hydrazine equilibration studies (Tests 7 and 8) revealed no formation of a hydrazinated complex with ferric nitrate. The TGA traces for these samples are similar to that of pure ferric nitrate decomposition (Tests 5 and 6). Further, the final decomposition product of hydrazinated ferric nitrate in batch method is pure hematite. Batch study results of the ferric nitrate system have indicated very little or no hydrazination reaction.

3.1.3. Ferrous Oxalate. Ferrous oxalate decomposes in two steps, both in air (Test 9) and nitrogen (Test 10) environments, as observed in the TGA (Figure 2c) with a weight loss of 54.4 and 56.2%, respectively (Table 1). In air, the end product is α-Fe_2O_3 at 260 °C, whereas in nitrogen, the final product is Fe_3O_4 at ∼300 °C as identified by the XRD (Figure 3). The two-step decomposition of $FeC_2O_4{\cdot}2H_2O$ is due to the dehydration and oxidative decomposition of the anhydrous oxalate, which ends up in the formation of Fe_3O_4 in nitrogen. However, in air, the Fe_3O_4 further reacts with oxygen to form thermodynamically stable α-Fe_2O_3 as the final product, preceded by metastable γ-Fe_2O_3 intermediate, as proposed in the literature[40,48–52]

$$FeC_2O_4{\cdot}2H_2O \xrightarrow{-2H_2O} FeC_2O_4 \underset{-CO_2}{\overset{-CO}{\longrightarrow}} FeO \underset{-H_2}{\overset{-H_2O}{\longrightarrow}}$$

$$Fe_3O_4 \xrightarrow{+O_2} \gamma\text{-}Fe_2O_3 \xrightarrow{\Delta} \alpha\text{-}Fe_2O_3$$

The hydrazinated ferrous oxalate decomposes in a single sharp step at 150 °C producing γ-Fe_2O_3 particles in air (Test 11) with a weight loss of 61.2% as observed by TGA analysis (Figure 2c). In a nitrogen atmosphere, a mixture of magnetic oxide is obtained at ∼430 °C by multiple-step decomposition (Test 12). A formula of $FeC_2O_4{\cdot}2N_2H_4$ is assigned for the hydrazine complex on the basis of the estimated hydrazine content of 31.4% and total weight loss of 61.2%, which agree well with the calculated values of 30.7 and 61.7%, respectively. A similar hydrazine complex is reported previously

reported in litrature.[53] The IR peak positions (Figure S2 in the Supporting Information) could be replicated in the present study, thereby, confirming the hydrazine complexation.[40,45,54] The thermal sequence of the decomposition of $FeC_2O_4 \cdot 2N_2H_4$ is similar to decomposition of $FeC_2O_4 \cdot 2H_2O$. The hydrazine released from the complex reacts with air, liberating the energy for the oxidative decomposition, whereas the moisture and nitrogen liberated as reaction byproducts provides the necessary environment to stabilize the γ-Fe_2O_3.

$$FeC_2O_4 \cdot 2N_2H_4 \xrightarrow{-2N_2H_4} FeC_2O_4 \xrightarrow[-CO_2]{-CO} FeO \xrightarrow[-H_2]{+H_2O}$$

$$Fe_3O_4 \xrightarrow{+O_2} \gamma\text{-}Fe_2O_3 \xrightarrow{\Delta} \alpha\text{-}Fe_2O_3$$

3.2. Aerosol Pyrolysis Studies. *3.2.1. Ferrous Acetate.* Aerosolized ferrous acetate was mixed with hydrazine hydrate in the preheater at 100 °C and then sent through the tubular furnace (FuAR) maintained at different temperatures. The product obtained at 100 °C was chemically analyzed and found to have a hydrazine content of ∼20%, and showed a weight loss trace similar to that obtained in the batch study (Tests 3 and 4). A mixture of amorphous and Fe_3O_4 was obtained as final product when decomposed at 300 °C in nitrogen atmosphere (Test 13). The product of decomposition in the nitrogen atmosphere at 500 °C (Test 14) was black magnetic Fe_3O_4 as revealed by XRD, consistent with the results obtained from batch study. A mixture of γ-Fe_2O_3 and α-Fe_2O_3 was obtained as the final product when decomposed in an oxidizing atmosphere (air) at 500 °C (Test 15) as revealed by XRD (Figure 4). Pure γ-Fe_2O_3 may be synthesized using this process with a better control of temperature and residence time inside the reactor. The synthesized particles by aerosol route are submicrometer-sized unagglomerated hollow spheres as observed in SEM image (Figure 5).

3.2.2. Ferric Nitrate. An aerosol generated from an aqueous solution of ferric nitrate (0.1 M) was decomposed in a furnace reactor (FuAR), with and without mixing with aerosolized hydrazine. The decomposition product of aerosolized ferric nitrate collected at 100 °C in air (Test 16) is amorphous in nature. The collected sample showed a diffuse TGA trace, with a total weight loss of 32.7% at ∼300 °C (Figure 2b). On the basis of TGA weight loss results, the molecular weight of the product is identified to be similar to that of goethite (α-FeOOH·H_2O). Formation of goethite type intermediate is also observed during the batch decomposition process. The decomposition product of the aerosolized ferric nitrate at 800 °C (Test 24) was α-Fe_2O_3 as identified by XRD (Figure 4).

On the other hand, product collected by decomposition of aerosolized hydrazinated ferric nitrate at ∼100 °C (Test 17) showed the formation of lepidocrocite (γ-FeOOH·H_2O; ICDD: 01−070−8045) type phase and hydrazine nitrate ($N_2H_5NO_3$; ICDD: 00−011−0197) as identified by XRD (Figure 4). TGA studies of the collected product showed a 76.0% weight loss at ∼270 °C with a sharp weight loss at ∼120 °C, amounting to >90% of total loss in both air and nitrogen (Figure 2b). The sharp weight loss at 120 °C is associated with the decomposition of $N_2H_5NO_3$, which releases a large amount of heat as reported in the literature.[55] The hydrazine estimation by KIO_3 on this decomposed product showed the presence of 18.7% hydrazine (in the form of $N_2H_5NO_3$). On the basis of TGA weight loss and hydrazine estimation and XRD analysis, formation of a γ-FeOOH·H_2O·$2N_2H_5NO_3$ type adduct is proposed, which supports the theoretical weight loss (73.1%) and hydrazine content (16.0% in the form of $N_2H_5NO_3$). Unlike batch studies, where no reaction between ferric nitrate and hydrazine vapors were observed, the formation of the hydrazine adduct is verified in the aerosolized state reaction. The total decomposition of aerosolized hydrazinated ferric nitrate led to the formation of γ-Fe_2O_3 between 300 - 550 °C (Tests 18−23), whereas thermodynamically stable α-Fe_2O_3 is the main product above 550 °C. The following reaction scheme is proposed on the basis of our studies where formation of structurally similar intermediate is found to be a key factor for the formation of γ-Fe_2O_3.

$$Fe(NO_3)_3 \cdot 9H_2O \xrightarrow{-6H_2O} Fe(NO_3)_3 \cdot 3H_2O \xrightarrow[-HNO_3]{+2N_2H_4}$$

$$\gamma\text{-}FeOOH \cdot H_2O \cdot 2N_2H_5NO_3 \xrightarrow{-2N_2H_5NO_3}$$

$$\gamma\text{-}FeOOH \cdot H_2O \xrightarrow{-1.5H_2O} 0.5\gamma\text{-}Fe_2O_3$$

3.2.3. Ferrous Oxalate. Iron oxalate and its hydrazine derivative are insoluble in water or in any most other solvents[55] and are unsuitable for aerosolization using the nebulizer setup. Thus, the iron oxalate and presynthesized $FeC_2O_4 \cdot 2N_2H_4$ (by equilibration method) was aerosolized using a fluidizer (not shown in experimental setup Figure 1) and decomposed at different temperature in FuAR. γ-Fe_2O_3 is obtained at 400 °C (Test 25) in air, whereas Fe_3O_4 is the end product at 500 °C in nitrogen atmosphere (Test 26) starting with $FeC_2O_4 \cdot 2N_2H_4$, similar to the results from the batch study. Interestingly, the aerosolized acicular

(46) Pattanayak, J.; Sitakara Rao, V.; Maiti, H. S. *J. Mater. Sci.* **1990**, *25*, 2245–2248.
(47) Delgado, E.; Bohórquez, A.; Pérez Alcázar, G.; Bolaños, A. *Hyperfine Interact.* **2003**, *148−149* (1−4), 129–134.
(48) Rane, K. S.; Nikumbh, A. K.; Mukhedkar, A. J. *J. Mater. Sci.* **1981**, *16* (9), 2387–2397.
(49) Hermanek, M.; Zboril, R.; Mashlan, M.; Machala, L.; Schneeweiss, O. *J. Mater. Chem.* **2006**, *16* (13), 1273–1280.
(50) Suzdalev, I. P.; Buravtsev, V. N.; Imshennik, V. K.; Maksimov, Y. V.; Matveev, V. V.; Volynskaya, A. V.; Trautwein, A. X.; Winkler, H. *Z. Phys. D* **1996**, *36* (2), 163–169.
(51) Rao, V.; Shashimohan, A. L.; Biswas, A. B. *J. Mater. Sci.* **1974**, *9*, 430–433.
(52) Venkataraman, A.; Mukhedkar, V. A.; Rahman, M. M.; Nikumbh, A. K.; Mukhedkar, A. J. *Thermochim. Acta* **1987**, *112*, 231–243.
(53) Cabanas, M. V.; Valletregi, M.; Labeau, M.; Gonzalezcalbet, J. M. *J. Mater. Res.* **1993**, *8* (10), 2694–2701.
(54) Shkodina, T. B.; Krylov, E. I.; Sharov, V. A. *Russ. J. Inorg. Chem.* **1972**, (2), 17.
(55) Miyake, A.; Kimura, A.; Ogawa, T.; Satoh, Y.; Inano, M. *J. Thermal Anal. Calorim.* **2005**, *80* (2), 515–518.

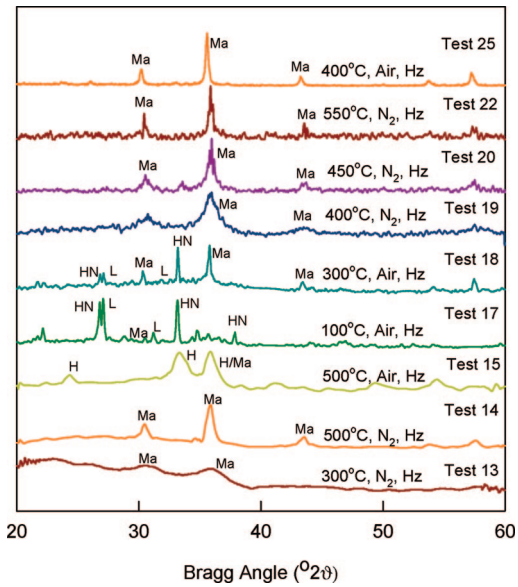

Figure 4. Characteristic X-ray diffraction patterns of the samples collected at outlet of the furnace aerosol reactor for various conditions (H, hematite; HN, hydrazine nitrate; L, lepidocrocite; Ma, maghemite; Hz, with hydrazine condition).

$FeC_2O_4 \cdot 2N_2H_4$ is topotactically decomposed to magnetic γ-Fe_2O_3 maintaining acicularity, supported by the SEM images (Figure 5).

4. Discussion: Overall Mechanism of Hydrazine-Assisted Synthesis

From the foregoing results of the thermal decomposition studies of ferrous acetate, ferric nitrate, and ferrous oxalate and their hydrazine derivatives, it is observed that in general, the addition of hydrazine plays multiple roles: modification of the decomposition pathway and the lowering of decomposition temperature to facilitate the formation of metastable γ-Fe_2O_3. Control of aerosol pyrolysis process parameters facilitate control of the particle size and morphology along with desired product crystallinity, which is otherwise very difficult to produce in single-step processes.

4.1 Hydrazine for Intermediate Adduct Formation. All iron precursors used in this study reacted to different #xb0rees with hydrazine vapor to form intermediate adducts. The chemical formula of the hydrazine adduct formed by ferrous acetate and ferrous oxalate is proposed as $Fe(CH_3COO)_2 \cdot 2N_2H_4$ and $FeC_2O_4 \cdot 2N_2H_4$, respectively, on the basis of the batch study, whereas that for ferric nitrate system is proposed as γ-$FeOOH \cdot H_2O \cdot 2N_2H_5NO_3$ based on aerosol pyrolysis study. The proposed structures are supported by the combined results of titration method, thermogravimetric analysis, infrared spectra and X-Ray diffraction analysis. It is found that the hydrazine-modified precursors decompose in a pathway different from the unhydrazinated precursors. A hexagonal goethite (α-$FeOOH \cdot H_2O$) type intermediate phase is formed during decomposition of the ferric nitrate, which led to formation of hexagonal α-Fe_2O_3. A cubic lepidocrocite (γ-$FeOOH \cdot H_2O$) type intermediate is identified during decomposition of aerosolized hydrazinated ferric nitrate, which led to formation of metastable cubic γ-Fe_2O_3. During hydrazine-assisted aerosol pyrolysis of ferrous acetate and ferrous oxalate, formation of metastable γ-Fe_2O_3 is preceded by structurally similar cubic intermediate (FeO and/or Fe_3O_4).

4.2. Hydrazine as Fuel: Lowering of Decomposition Temperature. From the results of the thermal decomposition studies of for both batch process and hydrazine-assisted aerosol pyrolysis process, it is observed that in general, the decomposition temperature is lowered by modifying the precursor with hydrazine. High-purity metastable γ-Fe_2O_3 can be synthesized from hydrazine modified ferrous acetate (Test 3) and ferrous oxalate (Test 11) at 320 and 150 °C, respectively, in a batch process, which is not possible without the hydrazination process (Table 1). Similarly, in hydrazine-assisted aerosol pyrolysis process, γ-Fe_2O_3 is synthesized from hydrazine-modified ferrous acetate (Test 15), ferric nitrate (Test 19−23) and ferrous oxalate (Test 25) precursors between 400 and 500 °C. The lowering of decomposition temperature may be attributed by the heat liberated by the exothermic reaction of hydrazine with oxygen. The hydrazine is released from the precursor particles ($Fe(CH_3COO)_2 \cdot 2N_2H_4$ and $FeC_2O_4 \cdot 2N_2H_4$) during decomposition and reacts with atmospheric oxygen ($N_2H_4 + O_2 \rightarrow N_2 + H_2O$, $\Delta H = -625$ kJ M^{-1}), liberating large amounts of localized energy. This localized transient energy surrounding the particle, along with a controlled supply of energy from an external source (by the furnace), enables the formation of metastable γ-Fe_2O_3. In case of the ferric nitrate system, the energy is supplied by the decomposition of $N_2H_5NO_3$ ($\Delta H = -256.5$ kJ M^{-1}) for low-temperature decomposition. Because the decomposition of $N_2H_5NO_3$ does not depend on the decomposition atmosphere, the γ-Fe_2O_3 can synthesized of nitrogen atmosphere, unlike other two systems. The reaction byproducts of hydrazine decomposition (nitrogen and water vapor) makes a protective layer surrounding each precursor particle, functioning as an individual aerosolized microreactor, thereby stabilizing γ-Fe_2O_3. Thus, lowering the decomposition temperature along with formation of inert surrounding atmosphere helps to restrict the further conversion of γ-Fe_2O_3 into α-Fe_2O_3.

4.3. Thermokinetic Comparison: Evolution of Phases. Decomposition temperatures of all the hydrazinated precursors are found to be higher in the aerosol pyrolysis method compared to the batch synthesis method. Reaction time and reaction temperature are identified as crucial factors that control the phase evolution during synthesis process. From a thermokinetic point of view, a process with long residence time in the reactor is expected to decompose at lower temperature or vice versa to produce the same final product. In the batch process, precursors were heated for a long duration (1 h) at a temperature close to their thermodynamic decomposition temperature (measured from TGA). However, during the aerosol pyrolysis process, because of a very short residence time inside the reactor (~8 s), a comparatively higher temperature is required to obtain the same final product. The optimal time−temperature history that is required varies from material to material and is primarily determined by intrinsic phase transition temperature characteristic of the system. As aerosol pyrolysis (without addition of hydrazine) is a high-temperature process, α-Fe_2O_3

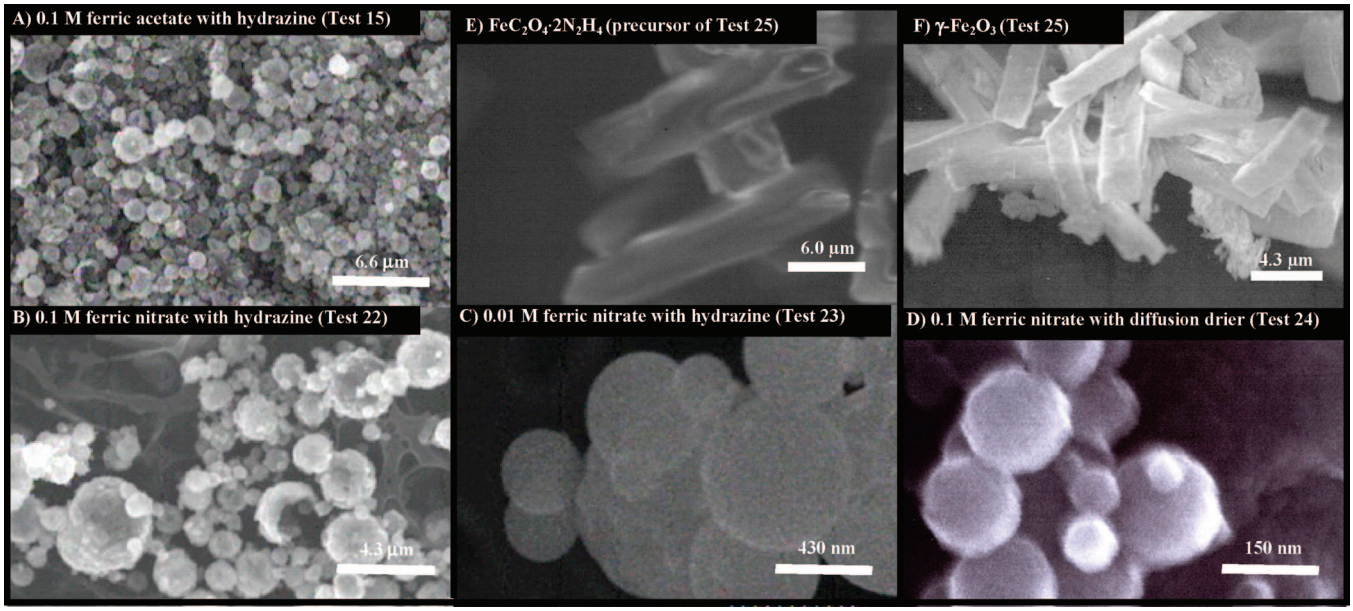

Figure 5. Characteristic scanning electron micrographs of the collected samples produced in the aerosol reactor illustrating different sizes, shapes, and morphology.

is typically the end product produced by this process when ferric nitrate is used as a precursor.[53] In the present study, the hydrazine-assisted, low-temperature aerosol pyrolysis of ferric nitrate as well as ferrous acetate are used for the successful production of metastable γ-Fe_2O_3.

Evolution of different phases is studied for the hydrazinated ferric nitrate system during the aerosol pyrolysis process. A goethite type (α-FeOOH·H_2O) phase was observed when aerosolized ferric nitrate was decomposed at 100 °C (Test 16). With a further increase in temperature, a hematite phase is produced at 800 °C (Test 24). On the other hand, hydrazine-assisted aerosol pyrolysis of ferric nitrate, lepidocrocite and hydrazine nitrate adduct (γ-FeOOH·H_2O·$N_2H_5NO_3$) is formed at 100 °C (Test 17). This adduct is found to be partially stable up to 300 °C in the furnace aerosol reactor, although the decomposition temperature of hydrazine nitrate is much lower (120 °C) because of the short residence time. The metastable maghemite type phase is first evolved at 300 °C (Test 18). Pure maghemite is produced between 400 and 550 °C in both air and nitrogen atmosphere, and α-Fe_2O_3 is the major product above 550 °C.

4.4. Control of Particle Size and Morphology. The particle size and morphology of the final product can be independently modified by hydrazine-assisted aerosol pyrolysis method without altering the crystallinity of the final product. The addition of hydrazine and control over decomposition temperature and reaction atmosphere are the main factors utilized to manipulate the crystal phase of the product. The morphology of the particles can be modified by alter in the evaporation rate of the aerosolized droplet before sending them into the furnace. The mean particle size can be varied by the changing the precursor concentration in the feed solution. Once the precursor is aerosolized and reacted with the hydrazine vapor, a diffusion drier is used to facilitate the evaporation rate of the moisture from the aerosolized droplet. Preliminary results show that the use of diffusion drier results in a solid spherical morphology, whereas absence of the diffusion drier produces a particle with a hollow spherical morphology. Two micrometer hollow spherical iron oxide (mixture of α-Fe_2O_3 and γ-Fe_2O_3) is produced (Figure 5a) by aerosolizing 0.1 M ferric acetate with hydrazine in the aerosol pyrolysis process (Test 15). Similarly, starting with a 0.1 M ferric nitrate solution, the formation of 2.0 μm hollow spherical γ-Fe_2O_3 particles (Test 22) and 120 nm solid spherical α-Fe_2O_3 (Test 24) is demonstrated in the present study, without and with use of diffusion drier, respectively (Figure 5). A lower starting precursor concentration (0.01 M) without diffusion drier (Test 23) has produced hollow spherical particles with a mean size of 400 nm (Figure 5). Further, micrometer-sized acicular shape γ-Fe_2O_3 particles are produced by the decomposition of the aerosolized hydrazinated ferrous oxalate (Test 25). In this case, the acicular shape of the solid precursor is topotactically decomposed to produce similar-shaped γ-Fe_2O_3 particles (Figure 5). Thus in general, a lower precursor concentration can produce smaller mean particle size, whereas use of the diffusion drier can change the morphology of the particles from hollow sphere to solid sphere as demonstrated in hydrozine-assisted aerosol pyrolysis methods.

5. Conclusions

The study of the thermal decomposition of various iron precursors and their hydrazine derivatives show that these decompose at lower temperatures compared to the pristine iron precursors and give better yields of γ-Fe_2O_3. Ferrous acetate and ferrous oxalate after equilibrating with hydrazine hydrate vapors form hydrazinated complexes, $Fe(CH_3COO)_2 \cdot 2N_2H_4$ and $FeC_2O_4 \cdot 2N_2H_4$ respectively, whereas ferric nitrate does not form such an adduct. Although in batch methods, ferric nitrate did not react with hydrazine hydrate vapor, the particles obtained at 100 °C from the aerosolized ferric nitrate and hydrazine hydrate in a FuAR indicated the likely formation of cubic lepidocrocite (γ-FeOOH·H_2O) type

intermediate phase. Decomposition reactions passing through a cubic intermediate (like FeO, Fe_3O_4, γ-$FeOOH \cdot H_2O$) are more likely to produce cubic γ-Fe_2O_3 as the final product because of their structural similarity. In situ supply of localized heat by coupled exothermic reaction of hydrazine with oxygen in a microreactor type environment, along with formation of a protective layer of nitrogen and moisture surrounding each particle allows for stabilizing the production of the metastable γ-Fe_2O_3. By tuning all the relevant parameters, it is possible to scale up this process and obtain uniform particle size distribution through hydrazine-assisted combustion spray pyrolysis with aqueous solutions of simple iron compounds.

Acknowledgment. We thank the National Science Foundation Nanoscale Exploratory Research award (BES-0608749) and The Center of Materials Innovation (CMI) at Washington University in Saint Louis for support of this work. K.S.R. thanks University Grants Commission (UGC), New Delhi, India, for financial assistance to Goa University for international collaboration under the UGC-Special Assistance Program.

Supporting Information Available: FT-IR traces (PDF). This material is available free of charge via the Internet at http://pubs.acs.org.

CM800034G